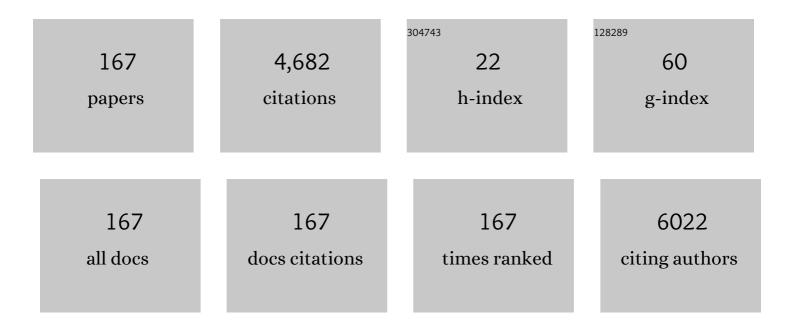
Alexander Wong

List of Publications by Year in descending order

Source: https://exaly.com/author-pdf/349182/publications.pdf Version: 2024-02-01



#	Article	IF	CITATIONS
1	VidAF: A Motion-Robust Model for Atrial Fibrillation Screening From Facial Videos. IEEE Journal of Biomedical and Health Informatics, 2022, 26, 1672-1683.	6.3	9
2	Computational and Experimental Model to Study Immunobead-Based Assays in Microfluidic Mixing Platforms. Analytical Chemistry, 2022, 94, 2087-2098.	6.5	1
3	Automated food intake tracking requires depth-refined semantic segmentation to rectify visual-volume discordance in long-term care homes. Scientific Reports, 2022, 12, 83.	3.3	14
4	BCUN: Bayesian Fully Convolutional Neural Network for Hyperspectral Spectral Unmixing. IEEE Transactions on Geoscience and Remote Sensing, 2022, 60, 1-14.	6.3	10
5	TAL: Topography-Aware Multi-Resolution Fusion Learning for Enhanced Building Footprint Extraction. IEEE Geoscience and Remote Sensing Letters, 2022, 19, 1-5.	3.1	4
6	Synthetic correlated diffusion imaging hyperintensity delineates clinically significant prostate cancer. Scientific Reports, 2022, 12, 3376.	3.3	4
7	Multi-Temporal Landsat-8 Images for Retrieval and Broad Scale Mapping of Soil Copper Concentration Using Empirical Models. Remote Sensing, 2022, 14, 2311.	4.0	5
8	A Bayesian Deep Image Prior Downscaling Approach for High-Resolution Soil Moisture Estimation. IEEE Journal of Selected Topics in Applied Earth Observations and Remote Sensing, 2022, 15, 4571-4582.	4.9	9
9	Hallway Gait Monitoring Using Novel Radar Signal Processing and Unsupervised Learning. IEEE Sensors Journal, 2022, 22, 15133-15145.	4.7	13
10	Understanding the temporal evolution of COVID-19 research through machine learning and natural language processing. Scientometrics, 2021, 126, 725-739.	3.0	46
11	Detecting Pulse Rates From Facial Videos Recorded in Unstable Lighting Conditions: An Adaptive Spatiotemporal Homomorphic Filtering Algorithm. IEEE Transactions on Instrumentation and Measurement, 2021, 70, 1-15.	4.7	11
12	OutlierNets: Highly Compact Deep Autoencoder Network Architectures for On-Device Acoustic Anomaly Detection. Sensors, 2021, 21, 4805.	3.8	9
13	Deep Neural Network Perception Models and Robust Autonomous Driving Systems: Practical Solutions for Mitigation and Improvement. IEEE Signal Processing Magazine, 2021, 38, 22-30.	5.6	9
14	EvoPose2D: Pushing the Boundaries of 2D Human Pose Estimation Using Accelerated Neuroevolution With Weight Transfer. IEEE Access, 2021, 9, 139403-139414.	4.2	22
15	POOF: Efficient Goalie Pose Annotation using Optical Flow. , 2021, , .		0
16	MANet: a Motion-Driven Attention Network for Detecting the Pulse from a Facial Video with Drastic Motions. , 2021, , .		2
17	Environment Classification for Robotic Leg Prostheses and Exoskeletons Using Deep Convolutional Neural Networks. Frontiers in Neurorobotics, 2021, 15, 730965.	2.8	39
18	Generative Adversarial Networks and Conditional Random Fields for Hyperspectral Image Classification, IEEE Transactions on Cybernetics, 2020, 50, 3318-3329	9.5	108

#	Article	IF	CITATIONS
19	COVID-Net: a tailored deep convolutional neural network design for detection of COVID-19 cases from chest X-ray images. Scientific Reports, 2020, 10, 19549.	3.3	1,784
20	An Innovative Eigenvector-Based Method for Traffic Light Scheduling. Journal of Advanced Transportation, 2020, 2020, 1-14.	1.7	2
21	Learn2Perturb: An End-to-End Feature Perturbation Learning to Improve Adversarial Robustness. , 2020, , .		29
22	Comparative Analysis of Environment Recognition Systems for Control of Lower-Limb Exoskeletons and Prostheses. , 2020, , .		14
23	A Deep Learning Approach for Multi-Depth Soil Water Content Prediction in Summer Maize Growth Period. IEEE Access, 2020, 8, 199097-199110.	4.2	19
24	ExoNet Database: Wearable Camera Images of Human Locomotion Environments. Frontiers in Robotics and AI, 2020, 7, 562061.	3.2	27
25	TimeConvNets: A Deep Time Windowed Convolution Neural Network Design for Real-time Video Facial Expression Recognition. , 2020, , .		8
26	Exploring the regional disc bulge response of the cervical porcine intervertebral disc under varying loads and posture. Journal of Biomechanics, 2020, 104, 109713.	2.1	3
27	Detecting Pulse Wave From Unstable Facial Videos Recorded From Consumer-Level Cameras: A Disturbance-Adaptive Orthogonal Matching Pursuit. IEEE Transactions on Biomedical Engineering, 2020, 67, 3352-3362.	4.2	12
28	Nonlocal Band-Weighted Iterative Spectral Mixture Model for Hyperspectral Imagery Denoising. IEEE Transactions on Geoscience and Remote Sensing, 2020, 58, 5588-5601.	6.3	3
29	EmotionNet Nano: An Efficient Deep Convolutional Neural Network Design for Real-Time Facial Expression Recognition. Frontiers in Artificial Intelligence, 2020, 3, 609673.	3.4	16
30	Global chlorophyll-a concentration estimation from moderate resolution imaging spectroradiometer using convolutional neural networks. Journal of Applied Remote Sensing, 2020, 14, .	1.3	12
31	A Novel Motion Plane-Based Approach to Vehicle Speed Estimation. IEEE Transactions on Intelligent Transportation Systems, 2019, 20, 1237-1246.	8.0	19
32	SISC: End-to-End Interpretable Discovery Radiomics-Driven Lung Cancer Prediction via Stacked Interpretable Sequencing Cells. IEEE Access, 2019, 7, 145444-145454.	4.2	13
33	STAR-Net: Action Recognition using Spatio-Temporal Activation Reprojection. , 2019, , .		25
34	The Feasibility of Automated Identification of Six Algae Types Using Feed-Forward Neural Networks and Fluorescence-Based Spectral-Morphological Features. IEEE Access, 2019, 7, 7041-7053.	4.2	22
35	GolfDB: A Video Database for Golf Swing Sequencing. , 2019, , .		36
36	Estimation Of Iron Concentration In Soil Of A Mining Area From Uav-Based Hyperspectral Imagery. , 2019, , .		5

#	Article	IF	CITATIONS
37	Prototyping the Automated Food Imaging and Nutrient Intake Tracking System: Modified Participatory Iterative Design Sprint. JMIR Human Factors, 2019, 6, e13017.	2.0	11
38	ST-IRGS: A Region-Based Self-Training Algorithm Applied to Hyperspectral Image Classification and Segmentation. IEEE Transactions on Geoscience and Remote Sensing, 2018, 56, 3-16.	6.3	47
39	Extracting aerobic system dynamics during unsupervised activities of daily living using wearable sensor machine learning models. Journal of Applied Physiology, 2018, 124, 473-481.	2.5	24
40	Deep Learning with Darwin: Evolutionary Synthesis of Deep Neural Networks. Neural Processing Letters, 2018, 48, 603-613.	3.2	15
41	Deep Learning-Driven Depth from Defocus via Active Multispectral Quasi-Random Projections with Complex Subpatterns. , 2018, , .		0
42	MPCaD: a multi-scale radiomics-driven framework for automated prostate cancer localization and detection. BMC Medical Imaging, 2018, 18, 16.	2.7	43
43	63-3: Real-time Spatial-based Projector Resolution Enhancement. Digest of Technical Papers SID International Symposium, 2018, 49, 831-834.	0.3	2
44	Quantification of cyanobacterial cells via a novel imaging-driven technique with an integrated fluorescence signature. Scientific Reports, 2018, 8, 9055.	3.3	20
45	Enhancement of morphological and vascular features in OCT images using a modified Bayesian residual transform. Biomedical Optics Express, 2018, 9, 2394.	2.9	23
46	Autonomous gait speed estimation using 24GHz FMCW radar technology. , 2018, , .		9
47	Unsupervised Bayesian Classification of a Hyperspectral Image Based on the Spectral Mixture Model and Markov Random Field. IEEE Journal of Selected Topics in Applied Earth Observations and Remote Sensing, 2018, 11, 3325-3337.	4.9	17
48	Simultaneous Projector-Camera Self-Calibration for Three-Dimensional Reconstruction and Projection Mapping. IEEE Transactions on Computational Imaging, 2017, 3, 74-83.	4.4	33
49	Deep Randomly-Connected Conditional Random Fields For Image Segmentation. IEEE Access, 2017, 5, 366-378.	4.2	5
50	An Enhanced Probabilistic Posterior Sampling Approach for Synthesizing SAR Imagery With Sea Ice and Oil Spills. IEEE Geoscience and Remote Sensing Letters, 2017, 14, 188-192.	3.1	4
51	Radiomics-based Prognosis Analysis for Non-Small Cell Lung Cancer. Scientific Reports, 2017, 7, 46349.	3.3	196
52	Non-contact hemodynamic imaging reveals the jugular venous pulse waveform. Scientific Reports, 2017, 7, 40150.	3.3	53
53	A Novel Bayesian Spatial–Temporal Random Field Model Applied to Cloud Detection From Remotely Sensed Imagery. IEEE Transactions on Geoscience and Remote Sensing, 2017, 55, 4913-4924.	6.3	22
54	Weakly Supervised Classification of Remotely Sensed Imagery Using Label Constraint and Edge Penalty. IEEE Transactions on Geoscience and Remote Sensing, 2017, 55, 1424-1436.	6.3	22

#	Article	IF	CITATIONS
55	Compensated Row-Column Ultrasound Imaging System Using Multilayered Edge Guided Stochastically Fully Connected Random Fields. Scientific Reports, 2017, 7, 10644.	3.3	8
56	Fully automated segmentation of prostate whole gland and transition zone in diffusion-weighted MRI using convolutional neural networks. Journal of Medical Imaging, 2017, 4, 1.	1.5	57
57	Spectral-spatial fusion model for robust blood pulse waveform extraction in photoplethysmographic imaging. Biomedical Optics Express, 2016, 7, 4874.	2.9	18
58	Estimating oxygen uptake and energy expenditure during treadmill walking by neural network analysis of easy-to-obtain inputs. Journal of Applied Physiology, 2016, 121, 1226-1233.	2.5	26
59	Bag of Bags: Nested Multi Instance Classification for Prostate Cancer Detection. , 2016, , .		5
60	Hierarchical Grouping Approach for Fast Approximate RGB-D Scene Flow. , 2016, , .		1
61	TIGGER: A Texture-Illumination Guided Global Energy Response Model for Illumination Robust Object Saliency. , 2016, , .		0
62	Laser Light-field Fusion for Wide-field Lensfree On-chip Phase Contrast Microscopy of Nanoparticles. Scientific Reports, 2016, 6, 38981.	3.3	6
63	Spatial probabilistic pulsatility model for enhancing photoplethysmographic imaging systems. Journal of Biomedical Optics, 2016, 21, 116010.	2.6	11
64	Fully Connected Continuous Conditional Random Field With Stochastic Cliques for Dark-Spot Detection In SAR Imagery. IEEE Journal of Selected Topics in Applied Earth Observations and Remote Sensing, 2016, 9, 2882-2890.	4.9	13
65	Sparse reconstruction of compressive sensing MRI using cross-domain stochastically fully connected conditional random fields. BMC Medical Imaging, 2016, 16, 51.	2.7	2
66	Auto-calibration of a projector-camera stereo system for projection mapping. Journal of the Society for Information Display, 2016, 24, 510-520.	2.1	4
67	NeRD: A Neural Response Divergence Approach to Visual Saliency Detection. IEEE Signal Processing Letters, 2016, 23, 1404-1408.	3.6	0
68	Numerical Demultiplexing of Color Image Sensor Measurements via Non-linear Random Forest Modeling. Scientific Reports, 2016, 6, 28665.	3.3	8
69	StochasticNet: Forming Deep Neural Networks via Stochastic Connectivity. IEEE Access, 2016, 4, 1915-1924.	4.2	20
70	Intrinsic Representation of Hyperspectral Imagery for Unsupervised Feature Extraction. IEEE Transactions on Geoscience and Remote Sensing, 2016, 54, 1118-1130.	6.3	22
71	Extraction of Endmembers From Hyperspectral Images Using A Weighted Fuzzy Purified-Means Clustering Model. IEEE Journal of Selected Topics in Applied Earth Observations and Remote Sensing, 2016, 9, 695-707.	4.9	12
72	Salient Region Detection Using Self-Guided Statistical Non-Redundancy in Natural Images. IEEE Access, 2016, 4, 48-60.	4.2	58

Alexander Wong

#	Article	IF	CITATIONS
73	Automatic tracking of pupillary dynamics from <i>in vivo</i> functional optical coherence tomography images. Computer Methods in Biomechanics and Biomedical Engineering: Imaging and Visualization, 2016, 4, 306-316.	1.9	0
74	Feasibility of long-distance heart rate monitoring using transmittance photoplethysmographic imaging (PPCI). Scientific Reports, 2015, 5, 14637.	3.3	33
75	Bayesian-based deconvolution fluorescence microscopy using dynamically updated nonstationary expectation estimates. Scientific Reports, 2015, 5, 10849.	3.3	13
76	Monte Carlo-based noise compensation in coil intensity corrected endorectal MRI. BMC Medical Imaging, 2015, 15, 43.	2.7	7
77	35.1: Distinguished Paper : Auto-Calibration for Screen Correction and Point Cloud Generation. Digest of Technical Papers SID International Symposium, 2015, 46, 507-510.	0.3	1
78	Stochastic color image segmentation using spatial constraints. , 2015, , .		1
79	Scalable multi-neighborhood learning for convolutional networks. , 2015, , .		0
80	Automated prostate cancer detection via comprehensive multi-parametric magnetic resonance imaging texture feature models. BMC Medical Imaging, 2015, 15, 27.	2.7	140
81	Oil spill candidate detection from SAR imagery using a thresholding-guided stochastic fully-connected conditional random field model. , 2015, , .		15
82	Feature Extraction for Hyperspectral Imagery via Ensemble Localized Manifold Learning. IEEE Geoscience and Remote Sensing Letters, 2015, 12, 2486-2490.	3.1	12
83	Prostate Cancer Detection via a Quantitative Radiomics-Driven Conditional Random Field Framework. IEEE Access, 2015, 3, 2531-2541.	4.2	32
84	Return of grid seams: A superpixel algorithm using discontinuous multi-functional energy seam carving. , 2015, , .		1
85	Homotopic non-local regularized reconstruction from sparse positron emission tomography measurements. BMC Medical Imaging, 2015, 15, 10.	2.7	2
86	Hyperspectral Image Denoising Using a Spatial–Spectral Monte Carlo Sampling Approach. IEEE Journal of Selected Topics in Applied Earth Observations and Remote Sensing, 2015, 8, 3025-3038.	4.9	19
87	Simultaneous Scene Reconstruction and Auto-Calibration Using Constrained Iterative Closest Point for 3D Depth Sensor Array. , 2015, , .		1
88	Quantitative features for computer-aided melanoma classification using spatial heterogeneity of eumelanin and pheomelanin concentrations. , 2015, , .		3
89	Dense Depth Map Reconstruction from Sparse Measurements Using a Multilayer Conditional Random Field Model. , 2015, , .		5
90	Lung Nodule Classification Using Deep Features in CT Images. , 2015, , .		227

#	Article	IF	CITATIONS
91	Depth Profilometry via Multiplexed Optical High-Coherence Interferometry. PLoS ONE, 2015, 10, e0121066.	2.5	2
92	Compensated Row-Column Ultrasound Imaging System Using Fisher Tippett Multilayered Conditional Random Field Model. PLoS ONE, 2015, 10, e0142817.	2.5	6
93	A Deep-Structured Conditional Random Field Model for Object Silhouette Tracking. PLoS ONE, 2015, 10, e0133036.	2.5	3
94	Combining rotation forests and adaboost for hyperspectral imagery classification using few labeled samples. , 2014, , .		1
95	Markov-chain Monte Carlo-based image reconstruction for streak artefact reduction on contrast-enhanced computed tomography. Computer Methods in Biomechanics and Biomedical Engineering: Imaging and Visualization, 2014, 2, 67-75.	1.9	Ο
96	Comparative study of feature space projection methods for hyperspectral image classification. , 2014, ,		0
97	Noise-compensated homotopic non-local regularized reconstruction for rapid retinal optical coherence tomography image acquisitions. BMC Medical Imaging, 2014, 14, 37.	2.7	1
98	Image saliency detection via multi-scale statistical non-redundancy modeling. , 2014, , .		10
99	Comparison of unsupervised segmentation methods for surficial materials mapping in Nunavut, Canada using RADARSAT-2 polarimetric, Landsat-7, and DEM data. , 2014, , .		Ο
100	URC: Unsupervised regional clustering of remote sensing imagery. , 2014, , .		2
101	Sea Ice Surface Temperature Estimation Using MODIS and AMSR-E Data Within a Guided Variational Model Along the Labrador Coast. IEEE Journal of Selected Topics in Applied Earth Observations and Remote Sensing, 2014, 7, 3685-3694.	4.9	4
102	Grid Seams: A Fast Superpixel Algorithm for Real-Time Applications. , 2014, , .		9
103	K-P-Means: A Clustering Algorithm of K "Purified―Means for Hyperspectral Endmember Estimation. IEEE Geoscience and Remote Sensing Letters, 2014, 11, 1787-1791.	3.1	15
104	A KPCA texture feature model for efficient segmentation of RADARSAT-2 SAR sea ice imagery. International Journal of Remote Sensing, 2014, 35, 5053-5072.	2.9	7
105	Correlating optical coherence tomography images with dose distribution in late oral radiation toxicity patients. Photonics & Lasers in Medicine, 2014, 3, .	0.2	1
106	ETVOS: An Enhanced Total Variation Optimization Segmentation Approach for SAR Sea-Ice Image Segmentation. IEEE Transactions on Geoscience and Remote Sensing, 2013, 51, 925-934.	6.3	20
107	Sparse Reconstruction of Breast MRI Using Homotopic <formula formulatype="inline"><tex Notation="TeX">\$L_0\$</tex </formula> Minimization in a Regional Sparsified Domain. IEEE Transactions on Biomedical Engineering, 2013, 60, 743-752.	4.2	28
108	Computerised system for measurement of muscle thickness based on ultrasonography. Computer Methods in Biomechanics and Biomedical Engineering, 2013, 16, 249-255.	1.6	5

#	Article	IF	CITATIONS
109	Unsupervised classification of sea-ice using synthetic aperture radar via an adaptive texture sparsifying transform. , 2013, , .		2
110	Unsupervised classification of agricultural land cover using polarimetric synthetic aperture radar via a sparse texture dictionary model. , 2013, , .		8
111	A novel 3D approach for the extraction of the wetting front in CT images of soil profiles. , 2013, , .		3
112	Tensor total variation approach to optical coherence tomography reconstruction for improved visualization of retinal microvasculature. Biomedical Optics Express, 2012, 3, 160.	2.9	2
113	Saliency detection via statistical non-redundancy. , 2012, , .		10
114	Extracting High-Level Intuitive Features (HLIF) for Classifying Skin Lesions Using Standard Camera Images. , 2012, , .		17
115	Multi-scale tensor vector field active contour. , 2012, , .		2
116	Multi-Scale Saliency-Guided Compressive Sensing Approach to Efficient Robotic Laser Range Measurements. , 2012, , .		8
117	Automatic system for 3D reconstruction of the chick eye based on digital photographs. Computer Methods in Biomechanics and Biomedical Engineering, 2012, 15, 141-149.	1.6	1
118	Difference of Circles Feature Detector. , 2012, , .		3
119	Perceptual Structure Distortion Ratio: An Image Quality Metric Based on Robust Measures of Complex Phase Order. , 2012, , .		1
120	Statistical Conditional Sampling for Variable-Resolution Video Compression. PLoS ONE, 2012, 7, e45002.	2.5	1
121	Hybrid Video Compression Using Selective Keyframe Identification and Patch-Based Super-Resolution. , 2011, , .		7
122	Comprehensive Analysis on the Effects of Noise Estimation Strategies on Image Noise Artifact Suppression Performance. , 2011, , .		4
123	Synthesis of Remote Sensing Label Fields Using a Tree-Structured Hierarchical Model. IEEE Transactions on Geoscience and Remote Sensing, 2011, 49, 2060-2070.	6.3	2
124	Shot Boundary Detection Using Genetic Algorithm Optimization. , 2011, , .		4
125	Stochastic Medium Access for Cognitive Radio Ad Hoc Networks. IEEE Journal on Selected Areas in Communications, 2011, 29, 770-783.	14.0	22
126	Enhanced Seam Carving via Integration of Energy Gradient Functionals. IEEE Signal Processing Letters, 2011, 18, 375-378.	3.6	68

#	Article	IF	CITATIONS
127	Efficient Globally Optimal Registration of Remote Sensing Imagery via Quasi-Random Scale-Space Structural Correlation Energy Functional. IEEE Geoscience and Remote Sensing Letters, 2011, 8, 997-1001.	3.1	3
128	Quasi-Monte Carlo Estimation Approach for Denoising MRI Data Based on Regional Statistics. IEEE Transactions on Biomedical Engineering, 2011, 58, 1076-1083.	4.2	19
129	Automatic Skin Lesion Segmentation via Iterative Stochastic Region Merging. IEEE Transactions on Information Technology in Biomedicine, 2011, 15, 929-936.	3.2	104
130	Fisher–Tippett Region-Merging Approach to Transrectal Ultrasound Prostate Lesion Segmentation. IEEE Transactions on Information Technology in Biomedicine, 2011, 15, 900-907.	3.2	6
131	Constrained Bayesian streak artifact reduction approach for contrast enhanced computed tomography imaging of the intervertebral disc. , 2011, 2011, 8487-90.		0
132	Multi-scale 3D representation via volumetric quasi-random scale space. , 2011, , .		0
133	Tensor vector field based active contours. , 2011, , .		4
134	NONPARAMETRIC SAMPLE-BASED METHODS FOR IMAGE UNDERSTANDING. Series in Computer Vision, 2011, , 137-153.	0.1	0
135	Dynamically optimized spatiotemporal prioritization for spectrum sensing in cooperative cognitive radio. Wireless Networks, 2010, 16, 889-901.	3.0	6
136	An Adaptive Monte Carlo Approach to Phase-Based Multimodal Image Registration. IEEE Transactions on Information Technology in Biomedicine, 2010, 14, 173-179.	3.2	3
137	IceSynth II: Synthesis of SAR Sea-Ice Imagery Using Region-Based Posterior Sampling. IEEE Geoscience and Remote Sensing Letters, 2010, 7, 348-351.	3.1	7
138	CPOL: Complex phase order likelihood as a similarity measure for MR–CT registration. Medical Image Analysis, 2010, 14, 50-57.	11.6	19
139	A new Bayesian source separation approach to blind decorrelation of SAR data. , 2010, , .		4
140	Remote sensing image synthesis. , 2010, , .		3
141	Mammogram Image Superresolution Based on Statistical Moment Analysis. , 2010, , .		0
142	Quasi-Random Scale Space Approach to Robust Keypoint Extraction in High-Noise Environments. , 2010, ,		1
143	General Bayesian estimation for speckle noise reduction in optical coherence tomography retinal imagery. Optics Express, 2010, 18, 8338.	3.4	165
144	Extended Knowledge-Based Reasoning Approach to Spectrum Sensing for Cognitive Radio. IEEE Transactions on Mobile Computing, 2010, 9, 465-478.	5.8	33

#	Article	IF	CITATIONS
145	Spectral variation constrained power spectral density estimation for wideband spectrum sensing. , 2010, , .		0
146	Prioritized Spectrum Sensing in Cognitive Radio Based on Spatiotemporal Statistical Fusion. , 2009, , .		6
147	JEDI: Adaptive Stochastic Estimation for Joint Enhancement and Despeckling of Images for SAR. , 2009, , .		2
148	SEC: Stochastic Ensemble Consensus Approach to Unsupervised SAR Sea-Ice Segmentation. , 2009, , .		2
149	Alignment of Confocal Scanning Laser Ophthalmoscopy Photoreceptor Images at Different Polarizations Using Complex Phase Relationships. IEEE Transactions on Biomedical Engineering, 2009, 56, 1831-1837.	4.2	3
150	A systematic approach to feature tracking of lumbar spine vertebrae from fluoroscopic images using complex-valued wavelets. Computer Methods in Biomechanics and Biomedical Engineering, 2009, 12, 607-616.	1.6	2
151	Stochastic Channel Prioritization for Spectrum Sensing in Cooperative Cognitive Radio. , 2009, , .		5
152	Adaptive Monte Carlo Retinex Method for Illumination and Reflectance Separation and Color Image Enhancement. , 2009, , .		10
153	IceSynth: An Image Synthesis System for Sea-Ice Segmentation Evaluation. , 2009, , .		3
154	Intervertebral Disc Segmentation and Volumetric Reconstruction From Peripheral Quantitative Computed Tomography Imaging. IEEE Transactions on Biomedical Engineering, 2009, 56, 2748-2751.	4.2	15
155	Shape-guided active contour based segmentation and tracking of lumbar vertebrae in video fluoroscopy using complex wavelets. , 2008, 2008, 863-6.		9
156	Illumination invariant active contour-based segmentation using complex-valued wavelets. , 2008, , .		4
157	Automatic registration of inter-band and inter-sensor images using robust complex wavelet feature representations. , 2008, , .		2
158	A perceptually adaptive approach to image denoising using anisotropic non-local means. , 2008, , .		13
159	Robust Edge Detection Based on Non-local Contribution of Local Frequency Characteristics. , 2008, , .		0
160	Efficient FFT-Accelerated Approach to Invariant Optical–LIDAR Registration. IEEE Transactions on Geoscience and Remote Sensing, 2008, 46, 3917-3925.	6.3	37
161	Deblocking of Block-Transform Compressed Images Using Phase-Adaptive Shifted Thresholding. , 2008, ,		2
162	An Iterative Approach to Improved Local Phase Coherence Estimation. , 2008, , .		7

An Iterative Approach to Improved Local Phase Coherence Estimation. , 2008, , . 162

#	Article	IF	CITATIONS
163	An adaptive Monte Carlo approach to nonlinear image denoising. , 2008, , .		3
164	Efficient nonlocal-means denoising using the SVD. , 2008, , .		86
165	Simultaneous multi-modal registration of multiple images based on multi-dimensional joint phase moment distributions. , 2008, , .		Ο
166	Phase-adaptive image signal fusion using complex-valued wavelets. , 2008, , .		0
167	A nonlocal-means approach to exemplar-based inpainting. , 2008, , .		122